4.3-4.4 - Receiver Functions

- What are receiver functions?
- What can they tell us about the Earth from the crust to mantle scale?
- Case Studies.
  - Hudson Bay
  - Ethiopia
  - Sierra Nevada
  - Mantle Transition Zone…

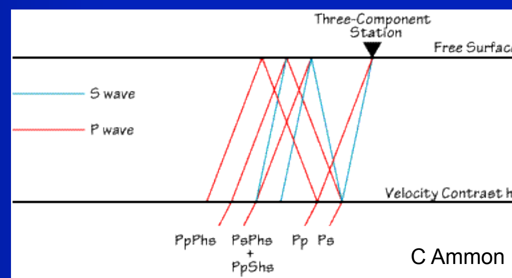

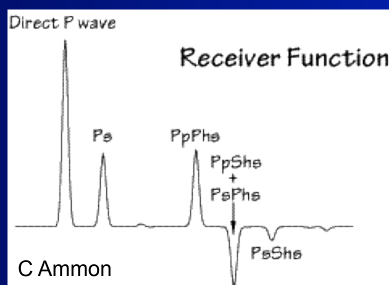

Ian Bastow, University of Bristol, UK

Receiver Functions – Overview

Receiver functions are time series, computed from three-component seismograms that show the response of Earth structure beneath a station. The waveform isolates P-to-S converted waves that reverberate in the structure beneath the seismometer.

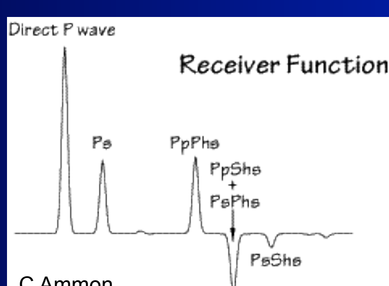

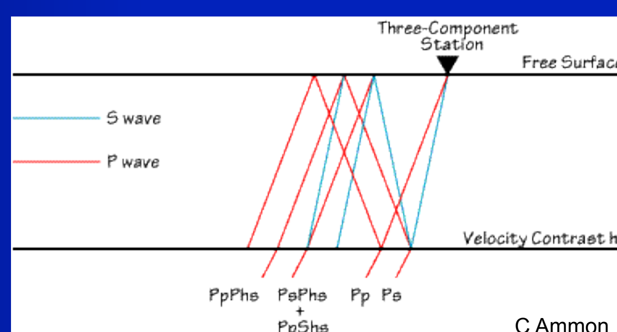

Modeling the amplitude and timing of the reverberations can provide valuable constraints on the underlying geology (H, Vp/Vs). The main features of the structure can be approximated by a sequence of horizontal layers and the arrivals generated by each sharp boundary looks something sketch on the right.

http://eqseis.geosc.psu.edu/~cammon/HTML/RftnDocs/rftn01.html

Receiver Functions – an Overview

Teleseismic arrival – steep angle of incidence beneath the station. Vertical component is dominated by P phases; horizontal components are dominated by converted S phases.

S(t) = STF(t) * P(t) * I(t) * H(t)

S: seismogram, ***STF***: earthquake source-time function, ***P***: along-path effects, ***I***: instrument response, ***H***: receiver function.

STF, ***P*** and ***I*** are common to all 3 seismogram components. P-to-S phases *should* only be on radial component.

Aim**:** to isolate the receiver function P-to-S converted phases that carry information about the station subsurface.

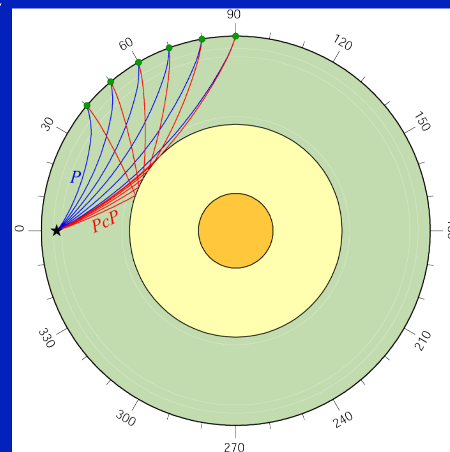

Receiver Function Computation

Isolate radial receiver function by deconvolving vertical component seismogram from radial (SV) component (same procedure for tangential, SH component). In the frequency domain:

$$H(w) = R(w) / Z(w),$$

Where w is the angular frequency $2\pi f$. Z(w) and R(w) are the Fourier Transforms of the vertical and radial seismograms. This is the “source equalization approach” E.g., Ammon, (1991).

A similar equation can be written for the tangential component of motion, defining the tangential receiver function.

This is a simple concept, but in reality, reliable implementation is difficult because of the instability of deconvolution.

Water Level Deconvolution (Langston, 1979)

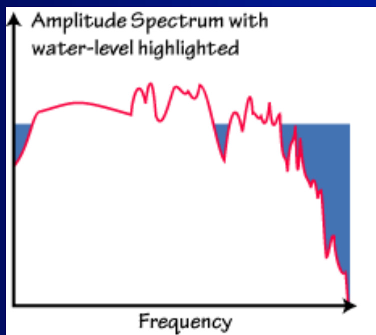

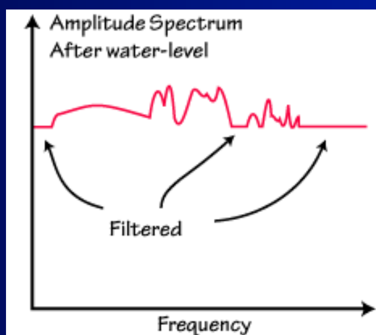

C. Ammon

- Small or zero values of Z(w) cause numerical problems in the calculation. There are several approaches to avoid this problem, the simplest is the ad hoc approach called water-level deconvolution. (Langston, 1979)

- Deconvolution includes a 'water-level' parameter to remove spectral holes, and the result is convolved with a Gaussian filter G(w):

$$H(w) = [R(w)\, Z^*(w) / Z(w)Z^*(w)]\, G(w).$$

Other Receiver Function Methods

Other methods include:

- Deconvolution in the time domain by least squares (e.g., Abers et al., 1995).
- Iterative deconvolution in the time domain (e.g., Ligorria & Ammon, 1999).
- Multi-taper frequency-domain cross-correlation receiver function (MTRF), Park & Levin (2000). **MTRF** is more resistant to noise so better for ocean island environments, for example. This advantage is due to the use of multitapers to minimize spectral leakage and its frequency dependent down-weighting in noisy portions of the spectrum.
- Helffrich (2006) further developed the **MTRF** method to focus on crustal and transition zone structures – **ETMTRF**: Extended Time Multitaper Frequency Domain Cross-Correlation Receiver Function Estimation.

What Receiver Functions can tell us about the Earth

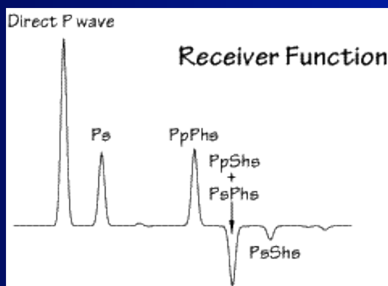

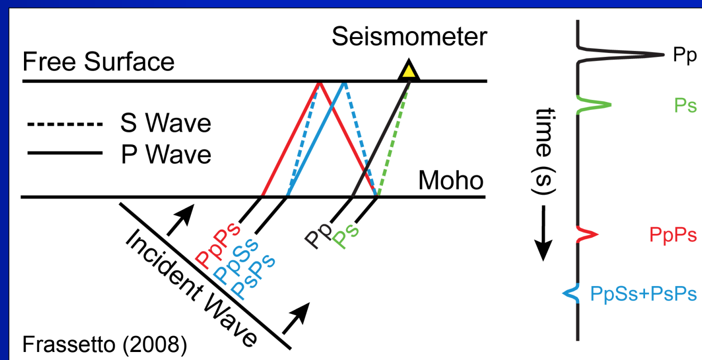

Example Receiver Function from Nunavut, northern Canada

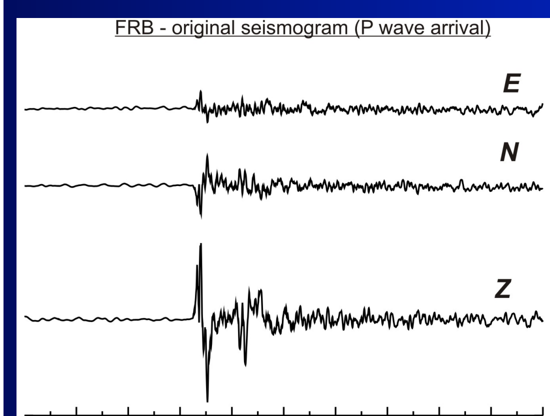

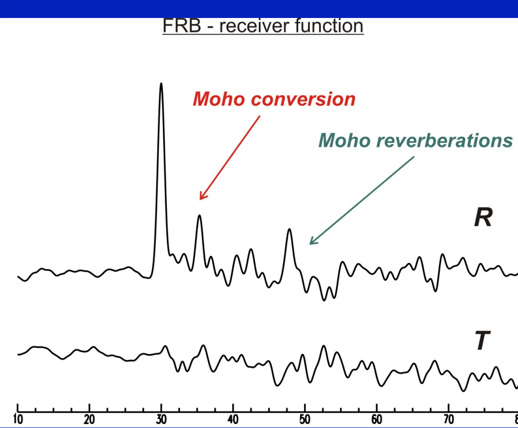

Case Study: Offshore Scottish Highlands

Comparisons with controlled source data

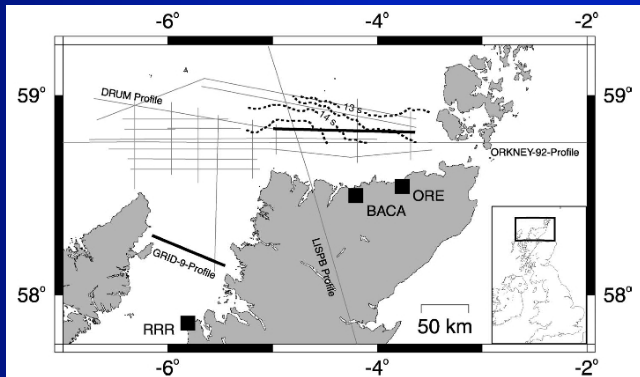

Figure 1. Location map of study area, showing (1) seismic stations (black squares); (2) location of deep seismic reflection profiles (eastern portion of DRUM and GRID-9 profiles shown in bold); and (3) contour (dotted line) of unmigrated two-way traveltimes to top of W reflector (contour interval 0.5 s).

Asencio et al., (2003)

Mantle Reflectors – the W and Flannan

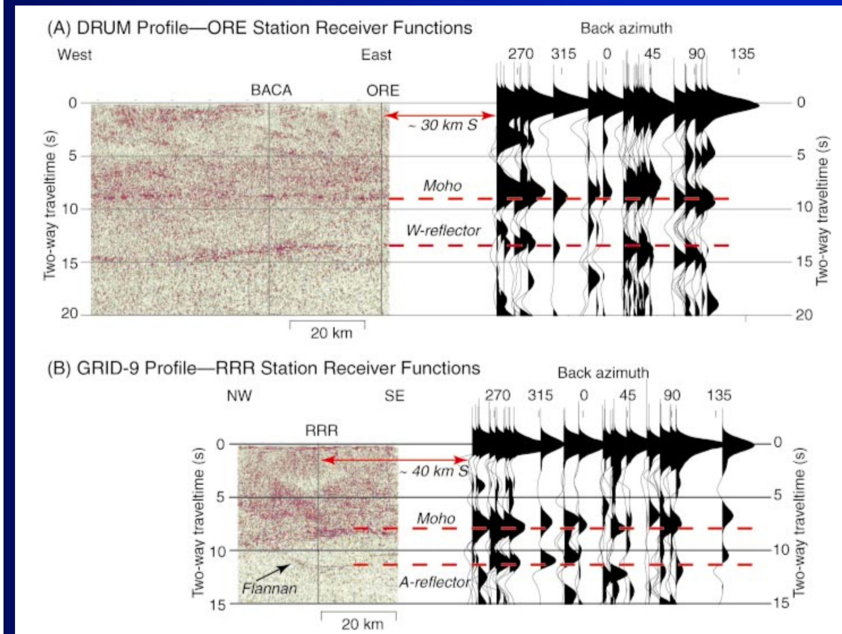

Figure 3. Correlation of radial component of receiver functions (as function of event back azimuth) at (A) ORE station with major reflectors on DRUM deep seismic reflection profile and (B) RRR station with major reflectors on GRID-9 deep seismic reflection profile. Vertical scale is two-way traveltime in seconds.

Asencio et al., (2003)

Case Study: The Sierra Nevada
Using Receiver Functions to Understand Lithospheric Foundering

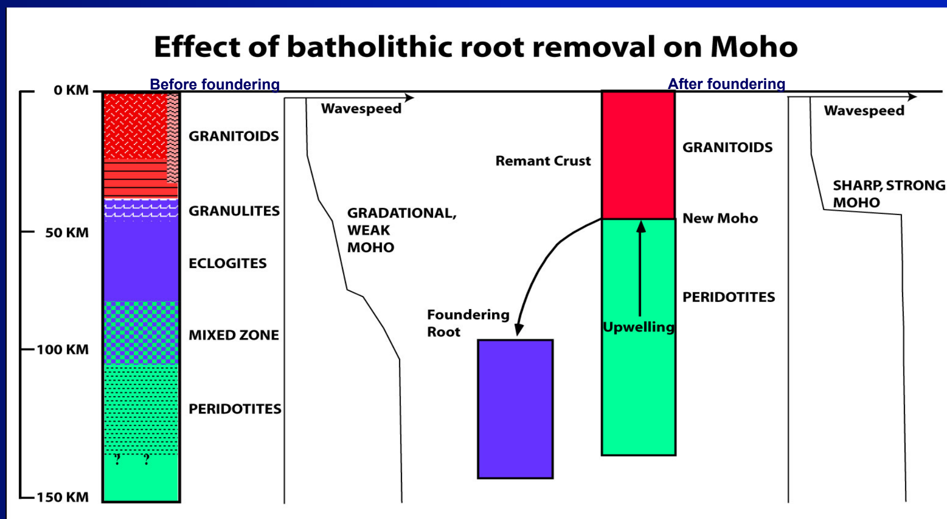

Image courtesy G. Zandt

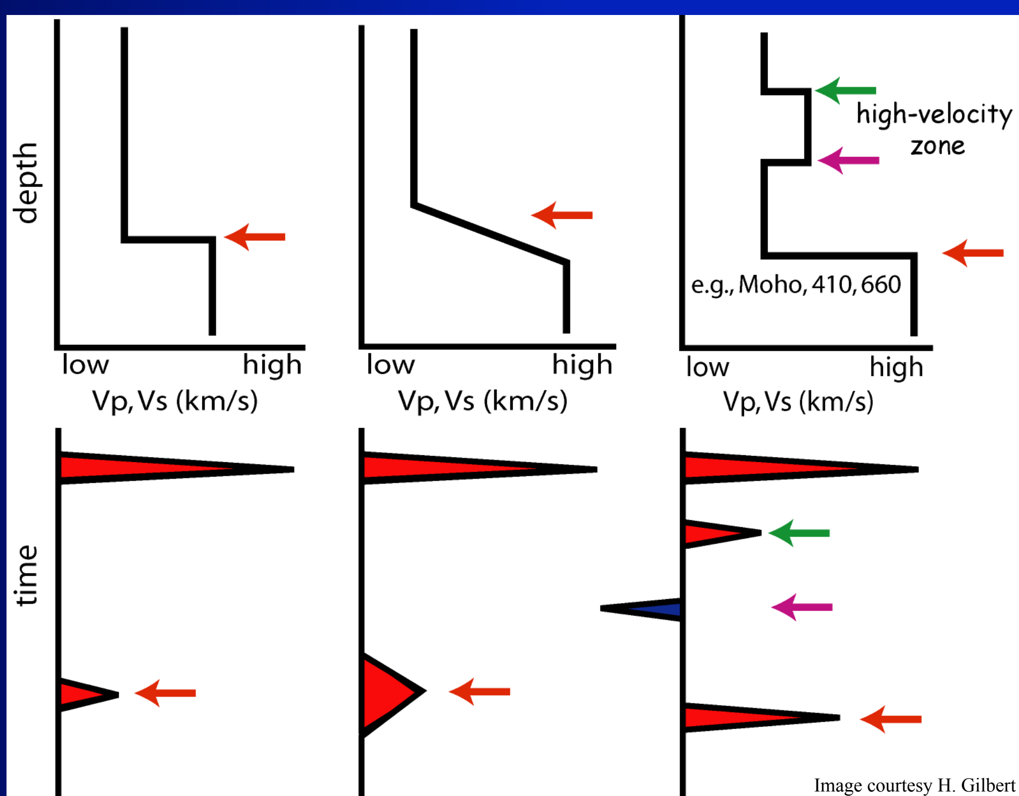

Image courtesy H. Gilbert

CCP Stacking

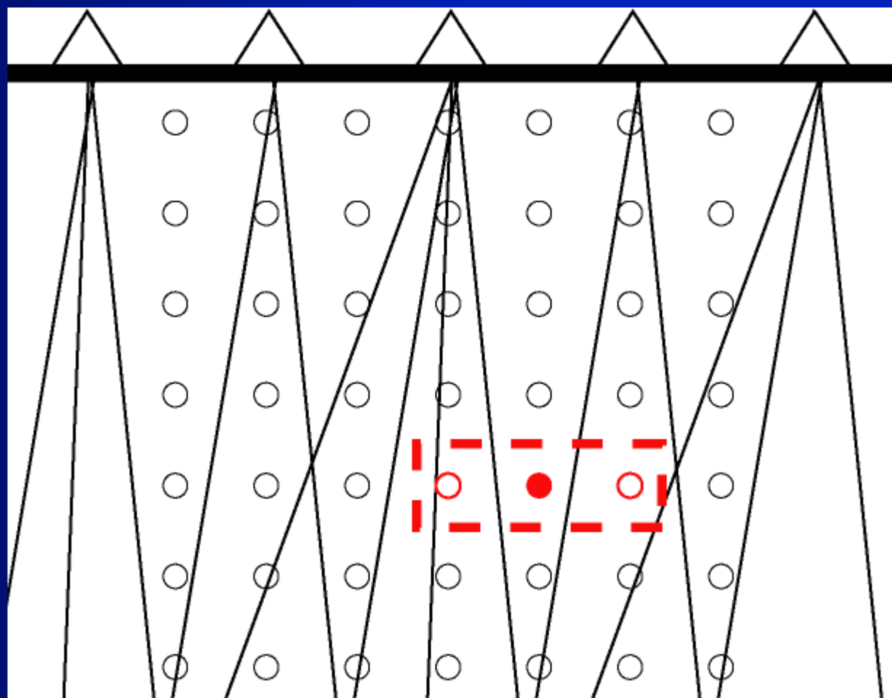

Frassetto et al., (2008)

Case Study – Cascadia Subduction Zone

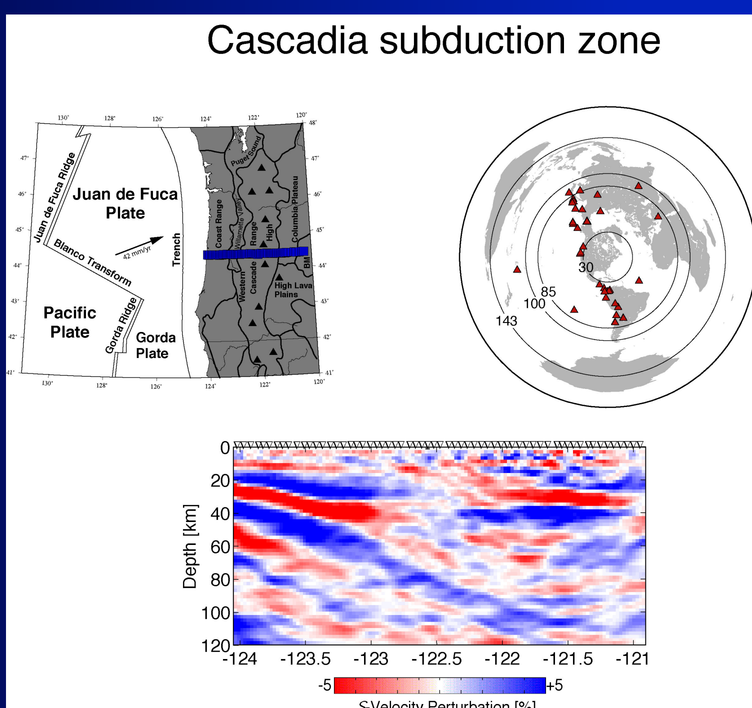

Rondenay et al., 2001

Calculate receiver function stacks for all stations along a dense array; carry out migration to convert time to depth → detailed images of subsurface discontinuities

Features: continental Moho, subducting Juan de Fuca slab, mineralogical changes (basalt to eclogite; different velocity properties)

Case Study: Imaging the Mantle Transition Zone With Receiver Functions

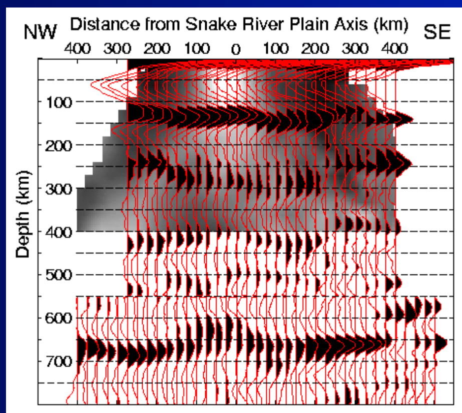

Dueker & Sheehan, 1997

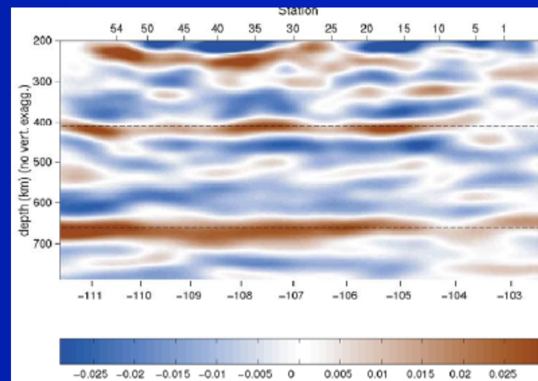

Wilson et al., 2005

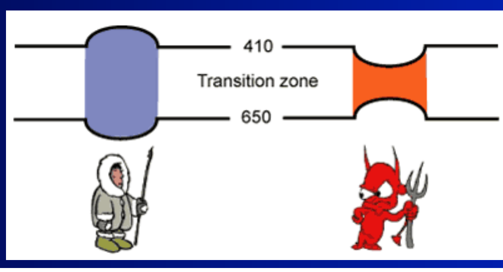

Discontinuities at ~410 km and ~660 km are strong enough to easily be imaged using single-station receiver functions and profile-based migrated sections. (Minor discontinuities also e.g. ~520 km)

Bulk Crustal Properties

- H-κ stacking method of Zhu & Kanamori (2000).
- Crustal thickness and Vp/Vs (κ) trade-off strongly.

$$t_1 = H\left[\sqrt{\frac{1}{V_S^2} - p^2} - \sqrt{\frac{1}{V_P^2} - p^2}\right]$$

$$t_2 = H\left[\sqrt{\frac{1}{V_S^2} - p^2} + \sqrt{\frac{1}{V_P^2} - p^2}\right]$$

$$t_3 = 2H\sqrt{\frac{1}{V_S^2} - p^2}$$

$$s(H,\kappa) = \sum_{j=1}^{N} w_1 r_j(t_1) + w_2 r_j(t_2) - w_3 r_j(t_3)$$

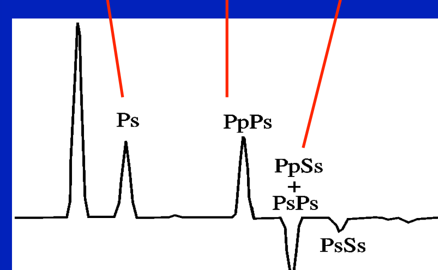

W1 (0.6), W2 (0.3), W3 (0.1) are weights.
Vp may be constrained by refraction data.
s(H,κ) should be a maximum at the correct H and Vp/Vs.

Ray Parameter P

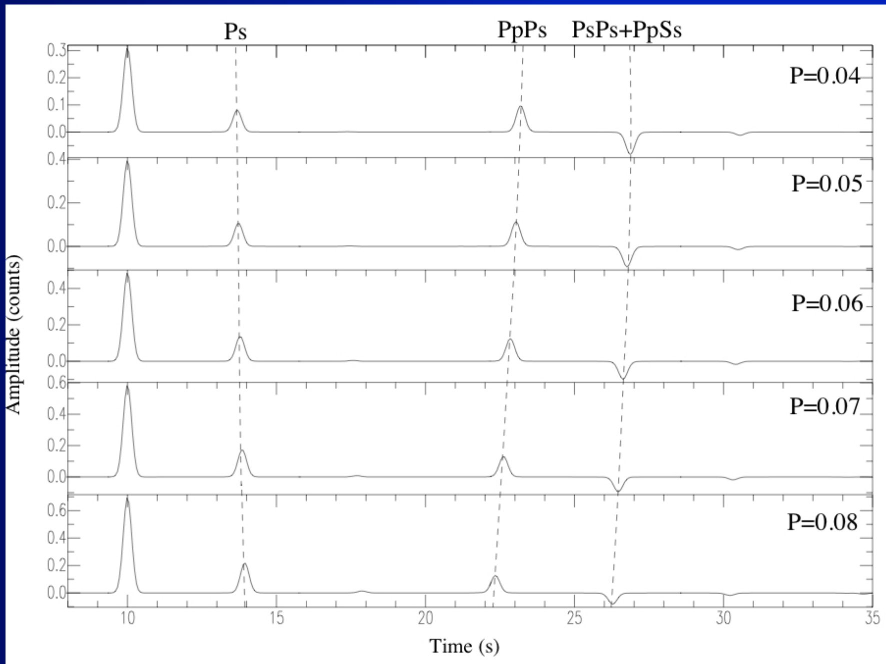

Epicentral Distance

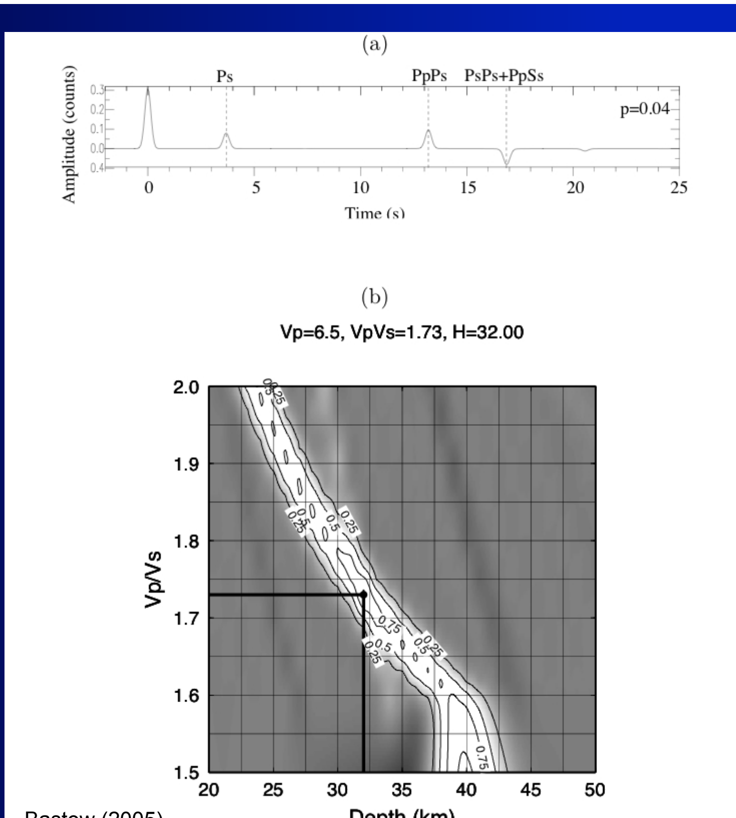

Bastow (2005)

Zhu & Kanamori (2000)

Bulk Crustal Properties H, Vp/Vs

$$\sigma = \frac{1}{2}\left[\frac{\left(\frac{V_P}{V_S}\right)^2 - 2}{\left(\left(\frac{V_P}{V_S}\right)^2 - 1\right)}\right]$$

Can relate Vp/Vs to Poisson's ratio.

Quartz: σ = 0.09

Plagioclaise Feldspar: σ = 0.3

Chevrot & Van der Hilst (2000)

The abundance of these minerals controls
bulk Poisson's ratio for many rocks.

Granite: 0.24

Diorite: 0.27

Gabbro: 0.30

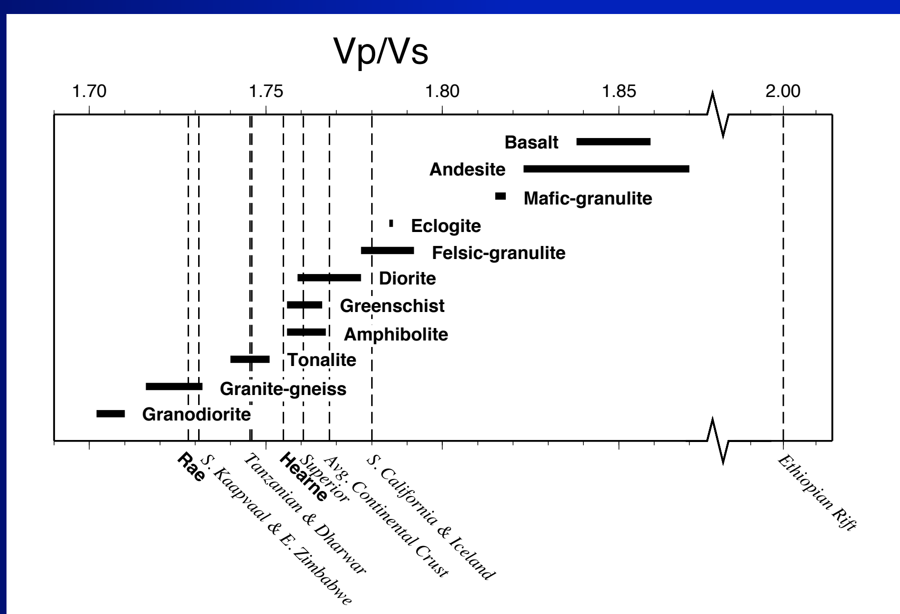

Thompson et al., (EPSL, 2010)

Case Study: The Ethiopian Rift

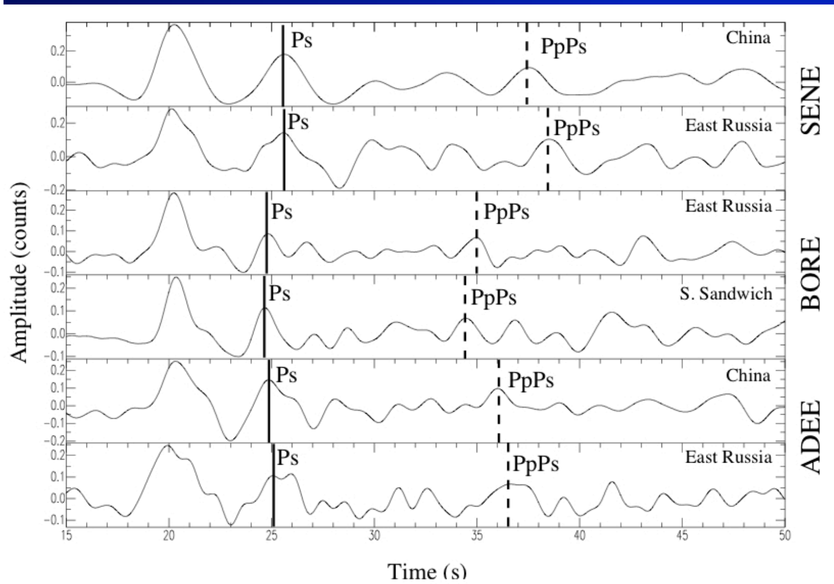

W. Plateau

Rift Valley

E. Plateau

Later arrivals at rift stations than plateau stations – crustal thickening.

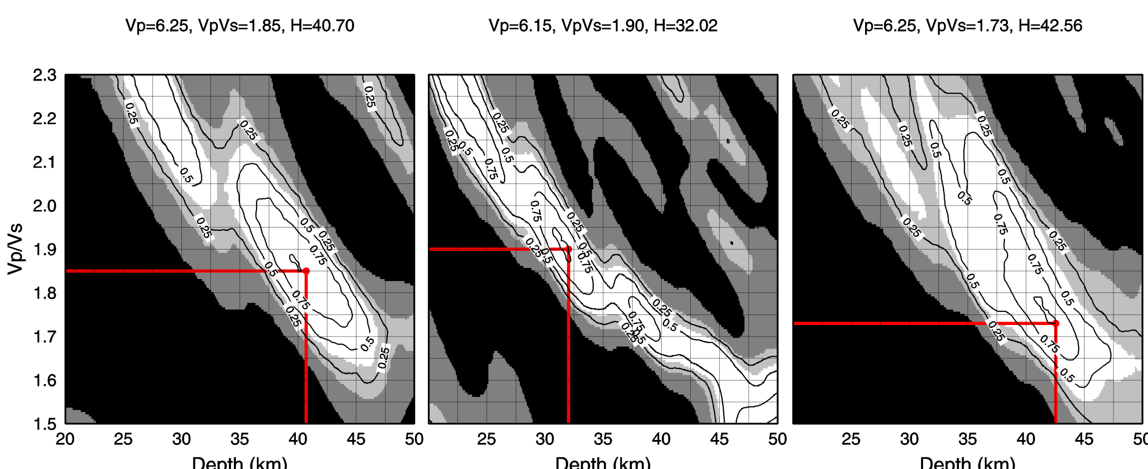

W. Plateau | Rift Valley | E. Plateau

- Vp/Vs higher in the rift than the plateaus. But lower to the E than to the W.
- Crustal thickness similar on the plateaus but (a little) thinner in the rift.

EARS

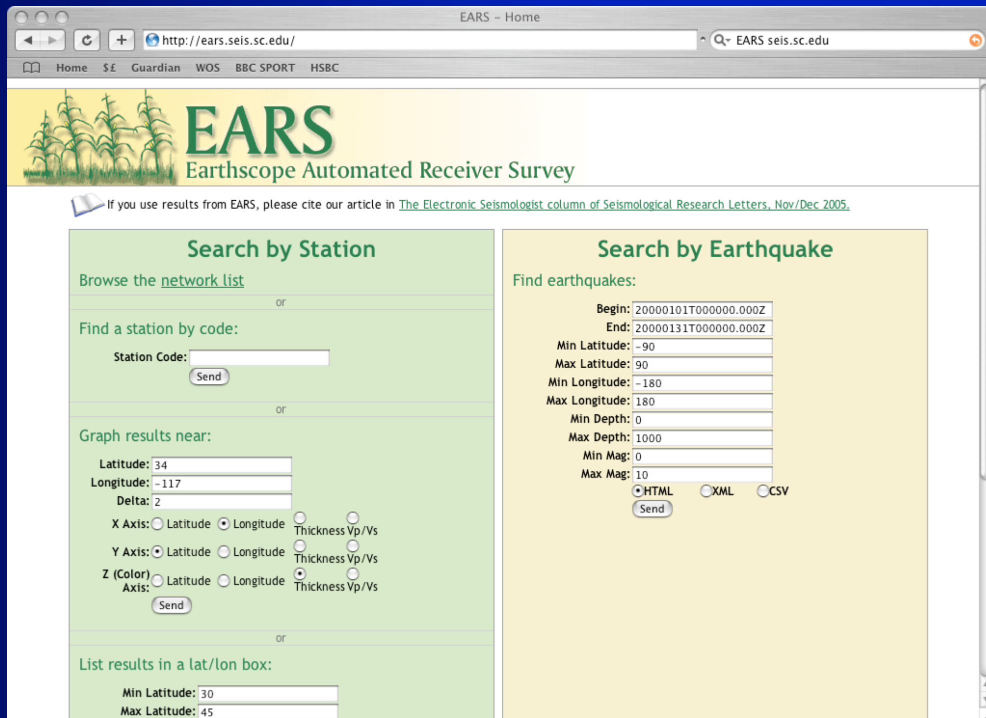

References

G.A. Abers, X. Hu, and L.R. Sykes. Source scaling of earthquakes in the Shumagin region, Alaska: time-domain inversions of regional waveforms. *Geophys. J. Int.*, 123(1):41–58, 1995.

C. J. Ammon, G. E. Randall, and G. Zandt. On the nonuniqueness of receiver function inversions. *J. Geophys. Res.*, 95(B10):15303–15318, 1990.

C.J. Ammon. The isolation of receiver effects from teleseismic *P* waveforms. *Bull., Seis. Soc. Am.*, 81(6):2504–2510, 1991.

E. Asencio, J.H Knapp, T.J. Owens, and G. Helffrich. Mapping fine-scale heterogeneities within the continental mantle lithosphere beneath Scotland: Combining active and passive source seismology. *Geology*, 31:447–480, 2003.

M.T. Dugda, A.A. Nyblade, J. Julià, C.A. Langston, C.A. Ammon, and S. Simiyu. Crustal structure in Ethiopia and Kenya from receiver function analysis. *J. Geophys. Res.*, 110(B1): doi:10.1029/2004JB003065, 2005.

G. Helffrich. Extended-Time Multitaper Frequency Domain Cross-Correlation Receiver-Function Estimation. *Bulletin of the Seismological Society of America*, 96(1):344–347, 2006.

C.A. Langston. Structure under Mount Rainer, Washington, inferred from teleseismic body waves. *J. Geophys. Res.*, 84:4749–4762, 1979.

J. Ligorrìa and C.J. Ammon. Iterative deconvolution and receiver-function estimation. *Bull., Seis. Soc. Am.*, 89(5):1395–1400, 1999.

T.J. Owens, A.A. Nyblade, and C.A. Langston. 410 and 660km discontinuity structure beneath Tanzania, East Africa. *Geophys. Res. Lett.*, 142:615–619, 2000.

J. Park and V. Levin. Receiver functions from multiple-taper spectral correlation estimates. *Bull., Seis. Soc. Am.*, 90(6):1507–1520, 2000.

M.E. Shaw Champion, N.J. White, S.M. Jones, and K.F. Priestley. Crustal velocity structure of the British Isles; a comparison of receiver functions and wide-angle seismic data. *Geophys. J. Int.*, 166(2):795–813, 2006.

G.W. Stuart, I.D. Bastow, and C.J. Ebinger. Crustal structure of the northern Main Ethiopian rift from reciever function studies, in The Structure and Evolution of the East African Rift System in the Afar Volcanic Province, eds. Yirgu, G. Ebinger, C.J. & Maguire, P.K.H. *Geol. Soc. Lond. Spec. Pub.*, 259:271–293, 2006.

L. Vinnik, V. Farra, and R. Kind. Deep structure of the Afro-Arabian hotspot by S receiver fuctions. *Geophys. Res. Lett.*, 31:doi: 10.1029/2004GL019574, 2004.

G. Zandt, H. Gilbert, T.J. Owens, M. Duceau, J. Saleeby, and C.H. Jones. Active foundering of a continental arc root beneath the southern Sierra Nevada in California. *Nature*, 43:41–46, 2004.

L. Zhu and H. Kanamori. Moho depth variation in southern California from teleseismic receiver functions. *J. Geophys. Res.*, 105(B2):2969–2980, 2000.

Some Useful References